Computational and Structural Biotechnology Journal 20 (2022) 3399–3408

COMPUTATIONAL ANDSTRUCTURAL BIOTECHNOLOGY JOURNAL

journal homepage: www.elsevier.com/locate/csbj

Macrophages and monocytes mediated activation of oxidative phosphorylation implicated the prognosis and clinical therapeutic strategy of Wilms tumour

Jialin Meng [a,b,c,1], Yonghao Chen [d,1], Xiaofan Lu [e,f,1], Qintao Ge [a,b,c], Feixiang Yang [a,b,c], Suwen Bai [g], Chaozhao Liang [a,b,c,*], Juan Du [g,*]

[a] Department of Urology, The First Affiliated Hospital of Anhui Medical University, Hefei 230022, Anhui, China
[b] Institute of Urology, Anhui Medical University, Hefei 230022, Anhui, China
[c] Anhui Province Key Laboratory of Genitourinary Diseases, Anhui Medical University, Hefei 230022, Anhui, China
[d] Department of Gastroenterology, West China Hospital of Sichuan University, Chengdu 610041, Sichuan, China
[e] State Key Laboratory of Natural Medicines, Research Center of Biostatistics and Computational Pharmacy, China Pharmaceutical University, Nanjing 211198, China
[f] Department of Cancer and Functional Genomics, Institute of Genetics and Molecular and Cellular Biology, CNRS/INSERM/UNISTRA, Illkirch 67400, France
[g] The Second Affiliated Hospital, School of Medicine, The Chinese University of Hong Kong, Shenzhen 518172, Guangdong, China

ARTICLE INFO

Article history:
Received 6 May 2022
Received in revised form 23 June 2022
Accepted 23 June 2022
Available online 27 June 2022

Keywords:
Nomogram
Tumor-infiltrating immune cells
Prognosis
Wilms tumor
Macrophages

ABSTRACT

Wilms tumour is the fourth leading cause of paediatric malignancy, but the detailed relationship between the tumour microenvironment and prognosis remains largely unclear. In this research, gene expression profile and clinical information from TARGET and the First Affiliated Hospital of Anhui Medical University were collected. After comparing the prognostic value of the associated immune cells, we established a nomogram to predict the prognosis of Wilms tumour based on monocyte infiltration, macrophage infiltration, stage, and sex. Further results showed that the most significant relationship between matrix metallopeptidase 9 and prognosis or macrophage infiltration. Meanwhile, by gene set enrichment or variation analyses and immunohistochemistry staining, we demonstrated that the most highly enriched hub genes were closely related to the activated oxidative phosphorylation pathway. Finally, through tumour immune dysfunction and an exclusion algorithm, the satisfactory discriminative performance of our nomogram was revealed for predicting the response to clinical therapy. Anti-PD1 therapy is more suitable for Wilms tumour patients with high nomogram points, and chemotherapies are more effective for patients with low nomogram score.

1. Introduction

Wilms tumour (WT, nephroblastoma), as the fourth leading cause of paediatric malignancy, accounts for approximately 500 new cases each year in the United States [1]. It has been identified by the National Wilms Tumor Society (NWTS) and the Children's Oncology Group (COG) as the most common kidney cancer in paediatric patients, with more frequency in girls than boys [1–3]. The latest data also show that the diagnosis of WT is often made in the first 3 years of life for sporadic cases and in 2 years for hereditary cases and is more common in Black children, but less common in Asian than in White children, emphasizing an important role of race and ethnic effects in the aetiology of WT [1,4]. WT can also occur along with genetic conditions and congenital syndromes in approximately 10% of cases, such as Denys-Drash syndrome, Wilms-Aniridia-Genitourinary-mental Retardation, and Beckwith-Wiedemann syndrome [5,6]. As reported by NWTS/COG and the International Society of Paediatric Oncology (SIOP), significant improvements in multimodal therapy have exceeded overall five-year survival rates by >90% in patients with localized disease [6–8]. Nevertheless, mortality continues to be a serious issue, especially for specific subgroups, including those who relapse, those with anaplastic histology, and those with bilateral tumours. These WT patients have shorter event-free survival time and are at risk for secondary neoplasms and other late complications [8].

* Corresponding authors at: The Second Affiliated Hospital, School of Medicine, The Chinese University of Hong Kong, Shenzhen 518172, Guangdong, China (J. Du). Department of Urology, The First Affiliated Hospital of Anhui Medical University, Hefei 230022, Anhui, China (C. Liang).

E-mail addresses: Liang_chaozhao@ahmu.edu.cn (C. Liang), dujuan@cuhk.edu.cn (J. Du).

[1] These authors contributed equally to the study.

https://doi.org/10.1016/j.csbj.2022.06.052

Tumour-infiltrating immune cells (TIICs) are essential components of the tumour microenvironment and could be promising candidates for disease prognosis and potential targets of immunotherapy, which can alter the immune status of tumours. The tumour microenvironment and immunotherapy effectiveness in WT have not been well understood until now, while the importance of TIICs and inflammatory and immune markers in other cancers has been well defined. Since 1972, nonmetastatic WT patients were observed to have stronger tumour-related cell-mediated cytotoxicity than patients with disseminated disease [9]. Another study reported that the $CD3^+$ $CD4^-$ $CD8^+$ T cell line was confirmed to be cytotoxic against HLA-$A2402^+$ WT cells [10]. Then, macrophage infiltration and few T lymphocytes were found in WT in Vakkila et al.'s incomplete study [11]. Holl et al. [12] reported activated $CD8^+$ and $CD4^+$ T cells present in WTs before and after chemotherapy, especially elevated levels of WT-infiltrating natural killer (NK) cells, compared with those from patients' peripheral blood cells. A high density of infiltrated $CD8^+$ lymphocytes at the invasive margin may play an important role in lowering recurrence [13]. Similarly, adaptive immune cells ($CD3^+$ T cells and $CD20^+$ B cells) were primarily localized in the stromal component of tumours, while the infiltration pattern and density of innate immune cells, such as $CD68^+$ tumour-associated macrophages (TAMs), myeloperoxidase-positive neutrophils, and mast cells, were distributed in all regions of the tumour [14,15]. The tight association between WT and immunocytes reflects the immune system's impact on tumorigenesis, as well as its predictive value.

A wide landscape of immune responses has been demonstrated based on a comprehensive understanding of TIICs. Until now, the expansive and comprehensive landscape of infiltrated TIICs in WT patients had not been elucidated, let alone the relationship between TIICs and prognosis. The newly developed computational approach CIBERSORT allows for immune cell profiling analysis based on the deconvolution of gene expression microarray data and an algorithm for in silico quantification [16]. The machine learning approach CIBERSORT uses a support vector regression, which allows us to identify immune cell-based prognostic and therapeutic markers more comprehensively and effectively. To construct a comprehensive overview of various immune cells and other factors, we hope our analysis will aid in the advent of novel prognostic factors and therapeutic targets for WT patients.

2. Materials and methods

2.1. Patient collection

Gene expression profile and clinical information of 130 wt patients and 6 healthy controls were collected from the TARGET-WT project [17]. Gene expression data for the fragments per kilobase of nonoverlapping exons per million fragments mapped (FPKM) were computed from the raw count form first and then converted into transcripts per kilobase million (TPM) data. Noise was defined as mRNAs with a TPM value <1 in over 90% of the samples and were removed. Slides fixed in formalin and embedded in paraffin (FFPE) were collected from seven WT patients who underwent tumourectomy at the First Affiliated Hospital of Anhui Medical University (AHMU-WT cohort). Clinical features and follow-up information of the seven patients were obtained by telephone or during consult in the clinic, and we used death as the end point.

2.2. Estimation of immunocytes infiltration

CIBERSORT, as a deconvolution algorithm analytical tool using a normalized gene signature matrix, was used to quantify the abundance, percentage, and cell composition of various TIICs [16]. The density and fractions of 22 subtypes of immune cells were defined by the LM22 signature file, including T cells [resting/activated memory CD4+ T cells, naïve $CD4^+$ T cells, follicular helper (Tfh) cells, regulatory T cells (Treg), $\gamma\delta$ T cells, CD8+ T cells], B cells (naïve B cells, memory B cells, plasma cells), macrophages (M0, M1, M2), NK cells (resting/activated), neutrophils, eosinophils, monocytes, dendritic cells (resting/activated) and mast cells (resting/activated). For the prognostic evaluation of immunocytes, the patients were separated into two groups via the median value of the proportion of each immunocyte.

2.3. Gene set enrichment analysis (GSEA) and gene set variation analysis (GSVA) analysis

A GSEA using the Kyoto Encyclopedia of Genes and Genomes (KEGG) pathways was performed to identify the significant potential molecular pathways in different WT groups [18]. Statistical significance was defined as a nominal P value of <0.05 and an FDR of <0.25. For gene sets that met the above criteria, cumulative effects were analysed, and vice versa. Among different gene sets, the adjusted normalized enrichment score (NES) was implemented for analysis. Then, GSVA was performed to establish and validate the activated signalling prognostic signature for WT. Diverse pathway enrichment scores were generated by a cumulative density function and Kolmogorov-Smirnov-like rank statistics.

2.4. Immune infiltration and immuno-/chemotherapeutic response prediction

The response to immunotherapy was evaluated by the Tumor Immune Dysfunction and Exclusion (TIDE) algorithm [19,20]. Additionally, a subclass analysis of 47 melanoma patients who underwent anti-cytotoxic T lymphocyte-associated protein 4 (anti-CTLA4) or anti-programmed death-1 (anti-PD1) therapies was performed to compare the similarity of expression profile to WT in different risk groups, representing the potential response to immunotherapy [21].

Additionally, we evaluated the response to chemotherapy for each patient with a public pharmacogenomics database, the Genomics of Drug Sensitivity in Cancer (GDSC) (https://www.cancerrxgene.org). Pazopanib, temsirolimus, and rapamycin, usually used for treating renal cell carcinoma, were chosen for the evaluation. Based on the GDSC data, the half-maximal inhibitory concentration (IC_{50}) was evaluated to observe the sensitivity of chemotherapeutics according to the "pRRophetic" package with 10-fold cross-validation [22].

2.5. Antibodies used for IHC

Formalin-fixed and paraffin-embedded WT sliced samples were collected from AHMU. CD14 (Anti-CD14 antibody, Cat. ab182032, Abcam Inc., Massachusetts, USA) and CD163 (anti-CD163 antibody, Cat. ab182422, Abcam Inc., Massachusetts, USA) were chosen to reflect the infiltration of monocytes and macrophages [23–27]. The expression level of MMP9 was examined by anti-MMP9 antibody (bs-0397R, Bioss Inc, Beijing, China). COX1 (anti-COX1 antibody: ab109025, Abcam Inc., Massachusetts, USA) and COX4 (anti-COX4 antibody: ab202554, Abcam Inc., Massachusetts, USA) were chosen to reflect the oxidative phosphorylation level. Following the same procedures as have been reported previously [28,29], positively stained cells were counted by ImageJ software (NIH, Bethesda, USA) [30].

2.6. Statistics

T-tests and Wilcoxon rank-sum tests were used for normally or nonnormally distributed data, respectively, to compare the continuous data from the two subtypes. Correlations between two continuous factors were conducted by the Pearson correlation test, and distribution differences between subgroups and predicted response to immunotherapy were analysed by the chi-square test. Time and status Cox regression analysis was conducted to construct the nomogram based on the "RMS" package, aiming to establish a predictive signature. Patients were separated into high-point (NomoH) and low-point (NomoL) groups for subsequent analysis via the points calculated by the nomogram. The differentially expressed genes (DEGs) between the NomoH and NomoL subgroups were selected by the "limma" package with the cut-off value of P < 0.05, |log2-fold-change| > 1. To select the calculation factors affecting prognosis and evaluate the predictive value of our nomogram, Kaplan-Meier (K-M) survival analysis based on overall survival (OS) was performed with the "survminer" package. Three-year and five-year survival rates were chosen as markers to judge the accuracy of our prediction model by calibration curve with the "RMS" package (bootstraps with 1000 resamples), and the Hosmer-Lemeshow (H-L) test was applied to detect the performance of fit for the nomogram. The receiver operating characteristic (ROC) curve was generated by the pROC package to assess the prediction ability, and the area under the curve (AUC) was recorded. Statistical significance was considered a two-sided P value <0.05. All analyses were completed by 3.6.5 R software (https://www.r-project.org).

3. Results

3.1. Identification of prognostic subsets of TIICs and correlated clinical indices for WT

The gene expression profile of 130 wt patients and 6 healthy controls were analysed based on the CIBERSORT algorithm. Detailed information on the CIBERSORT results for Wilms tumours and controls is presented in Table S1, and Fig. 1A provides a summary of the proportions of TIICs. To reveal detailed information, we compared the proportion of each type of TIIC among patients and controls (Fig. 1B). In general, $CD4^+$ T cells, dendritic cells, neutrophils, NK cells, and regulatory T cells were highly present in normal tissues. The infiltrated macrophages were higher in WT tissues than that in normal tissues ($P < 0.05$, Fig. 1B). We evaluated the predicted value of 14 types of immunocytes via K-M survival analysis and revealed that the infiltration of monocytes played a protective role (Fig. 1C, $P = 0.011$), while the infiltration of macrophages was a risk factor (Fig. 1D, $P = 0.013$). The polarized infiltration of other immunocytes did not lead to different OS outcomes (Fig. S1). In addition, we also evaluated the predictive value of several clinical characteristics and revealed that the age of the patients (Fig. 1E, $P = 0.75$) and tumour histology (Fig. 1F, $P = 0.67$) did not impact the prognosis, but males had a poor prognosis (Fig. 1G, $P = 0.039$), as did patients with advanced tumour stages (Fig. 1H, $P = 0.00011$).

Establishment and validation of a novel WT prognostic prediction nomogram.

A prognostic nomogram was built after the implementation of multivariable logistic regression analysis and is displayed in Fig. 2A. Our nomogram estimating 3- and 5-year survival rates for patients suffering from WT showed that the stage was the largest contributor to patient outcomes, followed by sex, monocytes, and macrophages. The points calculation system overlaying analytical prognostic factors based on the nomogram was positively correlated with the risk of death (Table S2, Fig. 2B). To compare the prognostic value of the nomogram, we separated the patients into two subgroups, and four subgroups along with the total points of patients calculated via the nomogram, and all obtained the results that the higher points, the poor OS (P < 0.0001, Fig. 2C). Thus, the application of nomogram system can provide valuable information in the prognostic prediction of WT. For further appraisal and evaluation, the accuracy of prognostic variables was evaluated by calibration analysis, the H-L test, and AUC value. Consistent H-L test statistics results in both the predicted-probability of 3-year (Fig. 2D, P = 0.760) and 5-year (Fig. 2E, P = 0.530) survival implied good calibration suggesting good fitting of the model. By measuring the AUC value, the results displayed favorable discrimination of the nomogram with an AUC of 0.758 in 3-year survival rate (Fig. 2F) and 0.741 in 5-year survival rate (Fig. 2G). We also compared the prognositc value of the newly defined nomogram with the clinical features of age, gender, tumor stage and histology type, observed that the nomogram showing the best predict value than others (Fig. 2H). To validate the prognostic point system, 7 patients from AHMU were enrolled and divided into NomoH or NomoL groups along with the nomogram-generated risk points. The clinicopathological characteristics of the 7 wt patients are presented in Table 1, and we separated the patients to high and low groups with the median value of the total point. Patients in the high group (n = 4) contained the points of 171.36; patients in the low group (n = 3) contained the points of 58.08 and 0. The IHC staining results for each patient sample are shown in Fig. S2. We found that a higher total point in WT was associated with a poor prognosis, while a lower level indicated a more prolonged OS (Fig. 2I, $P = 0.1362$). Some clinical parameters reported to be relevant to prognosis (neutrophil to lymphocyte ratio (NLR), platelet to lymphocyte ratio (PLR) and systemic immune-inflammation index (SII)) were derived from the clinical records, and the higher value of these indices in the NomoH group demonstrated the clinical usefulness of the generated nomogram (Fig. 2J).

3.2. Identification of key genes and signalling pathways associated with WT prognosis

We first evaluated the DEGs and determined that MMP9 showed the most notable difference between the two subgroups (Fig. 3A, Table S3), which was also verified in the violin plot with distinctive upregulation in the NomoH subgroup ($P = 0.007$, Fig. 3B). Meanwhile, a high level of MMP9 expression was related to a worse survival probability (Fig. 3C, $P = 0.041$) and positively correlated with macrophage infiltration (Fig. 3D, R = 0.64, $P < 0.001$). To increase the credibility of our prediction, IHC staining was conducted and confirmed an elevated MMP9 protein level in the NomoH subgroup from the AHMU-WT cohort (Fig. 3E).

GSEA demonstrated that the most enriched hub genes in the NomoH subgroup were closely related to the activated oxidative phosphorylation pathway (NSE = 1.676, $P = 0.036$), followed by the ribosome pathway (NSE = 1.643, $P = 0.054$) (Fig. 4A). Gene expression data from patients in the NomoL subgroup were associated with the activated pathways of vasopressin-regulated water reabsorption (NSE = 1.734, $P = 0.002$) and glycosaminoglycan degradation (NSE = 1.732, $P = 0.01$) (Fig. 4B). Furthermore, GSVA results indicated a similarly enriched oxidative phosphorylation pathway in the NomoH subgroup and an activated glycolysis signalling pathway in the NomoL subgroup (Fig. 4C). To validate the involvement of the activated oxidative phosphorylation pathway in the NomoH subgroup, we evaluated the protein level of cytochrome *C* oxidase submit 1/4 (COX1/4) in NomoH patient samples from the AHMU-WT cohort and observed extremely increased protein levels of COX1 (Fig. 4D).

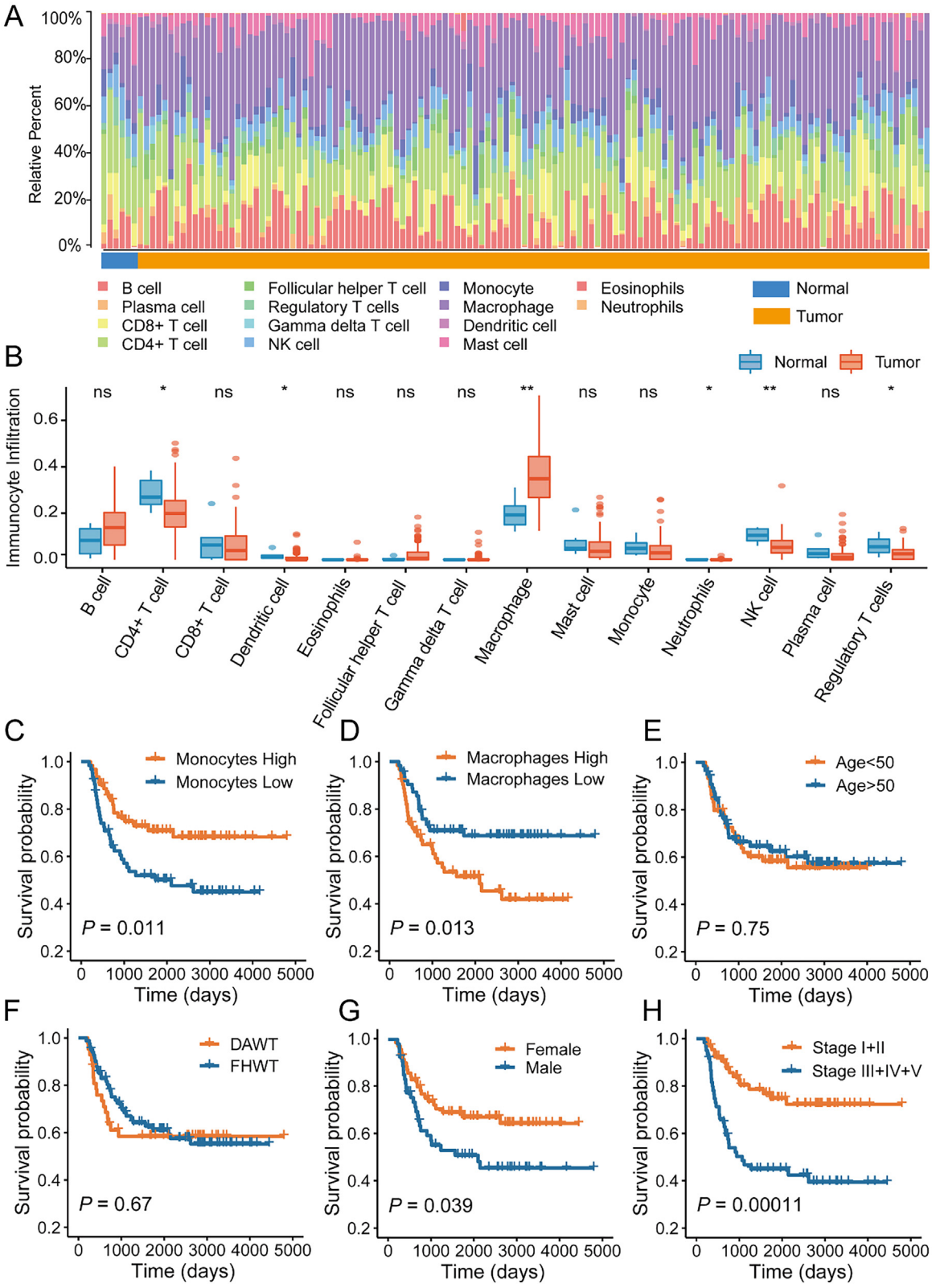

Fig. 1. Infiltration and prognostic value of immunocytes in WT. A, The overall distribution of immunocytes by CIBERSORT. B, Detailed distribution of different TIIC subtypes in the normal and tumour groups. C–H, K-M survival curves based on markedly different distributed TIICs and correlated clinical characteristics for prognostic analysis.

3.3. Exploration of an effective therapeutic strategy for WT patients

An estimation of the potential reaction to immunotherapy was implemented by the TIDE algorithm, and the outcomes suggested that patients in the NomoH subgroup were more likely to respond to immunotherapy ($P = 0.030$, Fig. 5A). Meanwhile, the nomogram risk points could also predict the response results of WT patients with reasonable accuracy (AUC = 0.633, Fig. 5B). After conducting

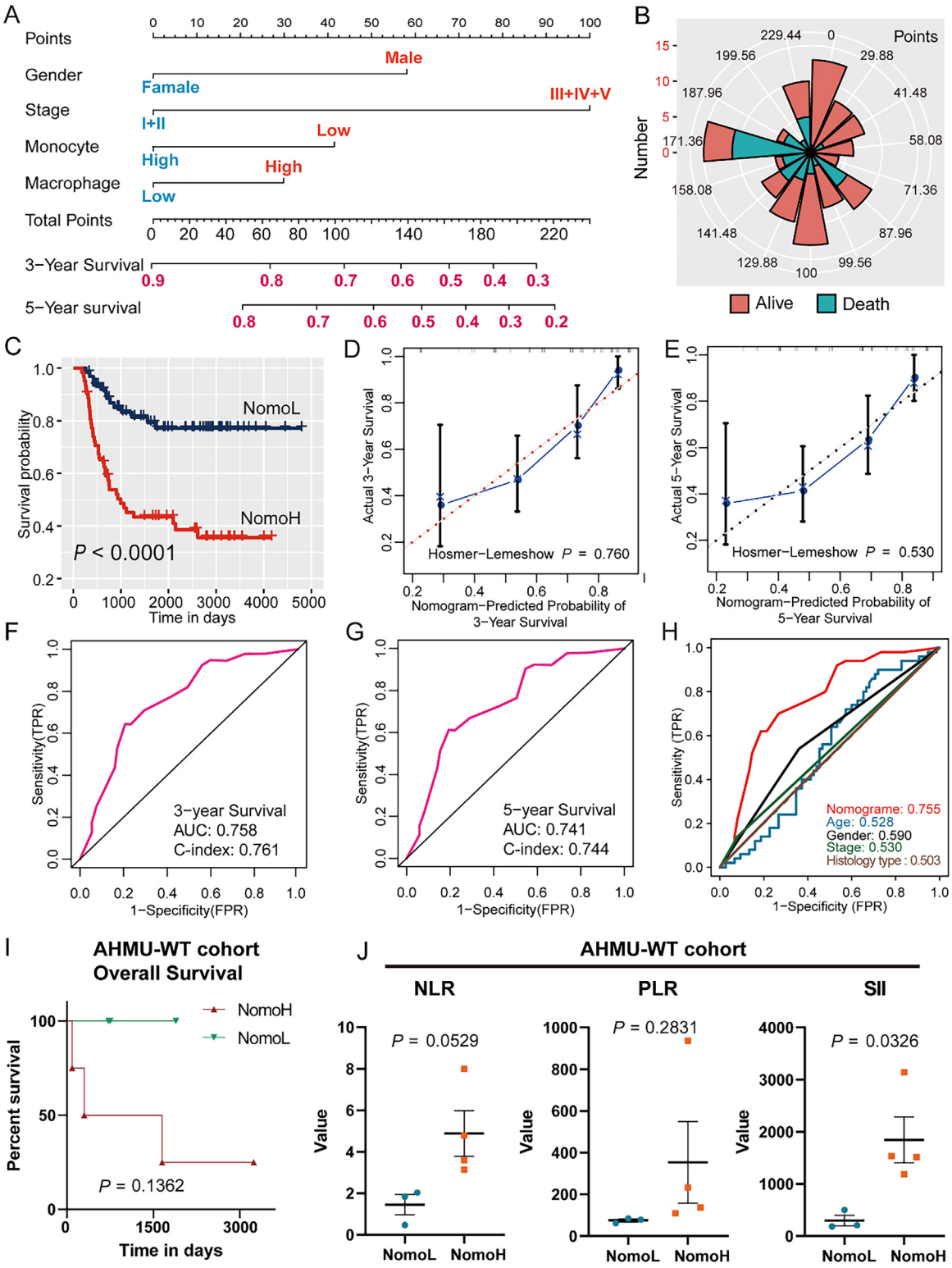

Fig. 2. Construction and validation of a prognostic nomogram. A, Nomogram for assessing the prognosis of WT patients. B, Point calculation system related to the risk of death. The points around the circle are calculated by the nomogram. C, K-M plot displaying the integrated value of survival probability (2 subgroups via the median value). D, Calibration curves and Hosmer-Lemeshow test for the validation of the predicted probability of 3-year survival. E, Calibration curves and Hosmer-Lemeshow test for the validation of the predicted probability of 5-year survival. F, ROC curve performed to estimates the predict performance of the nomogram (3 years). G, ROC curve performed to estimates the predict performance of the nomogram (5 years). H, ROC curve showing the prognostic value comparison between nomogram and clinical parameters. I, K-M plot validating the predictive value of the nomogram in seven real-world patients. J, The different distributions of clinical predictive factors (NLR, PLR, SII) between groups.

the submap analysis based on 47 melanoma patients who underwent anti-CTLA4 or anti-PD1 therapies and matching the expression profile, we revealed that patients in the NomoH subgroup were more likely to benefit from anti-PD1 therapy than those in the NomoL subgroup (Bonferroni corrected $P = 0.024$, Fig. 5C).

Table 1
Clinicopathological characteristics of Seven Wilms tumor patients.

Patient ID	Gender	Age, Months	Stage	Metastasis*	Status	Time#, Months	Monocyte Group	Macrophage group	Nomogram Points
1,200,732	Female	36	III	No	Alive	108	Low	High	171.36
1,322,706	Female	12	III	No	Dead	2	Low	High	171.36
1,605,177	Female	24	II	No	Dead	55	Low	High	171.36
1,815,146	Female	36	III	No	Dead	10	Low	High	171.36
1,523,492	Male	36	II	No	Alive	63	High	Low	58.08
1,824,171	Female	12	I	No	Alive	25	High	Low	0.00
1,831,478	Female	2	III	No	Alive	24	High	Low	0.00

*, Including metastasis to node, adrenal gland, and ureter; #, Overall survival time or follow-up time.

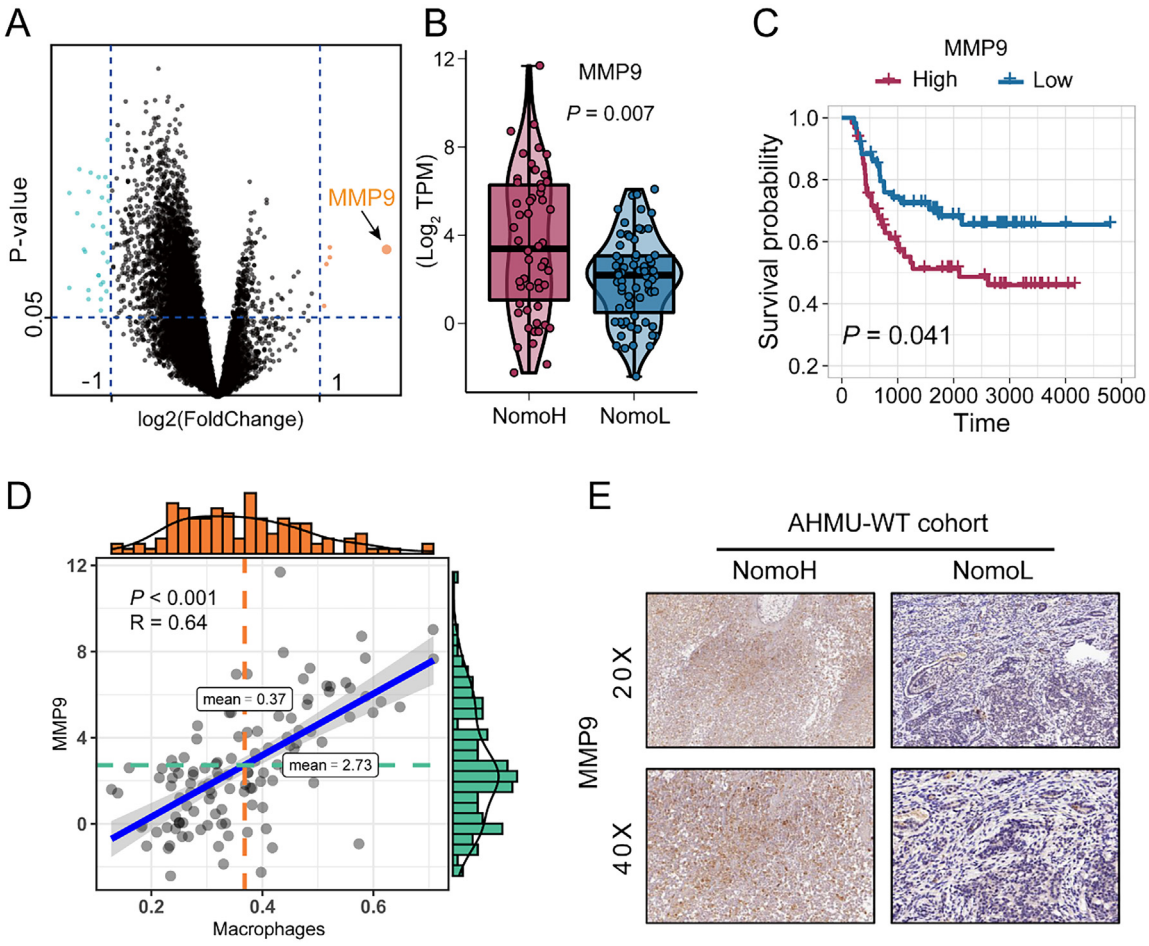

Fig. 3. MMP9 promotes the poor prognosis of WT patients. A, Volcano plot showing DEGs between the NomoH and NomoL subgroups. B, Differential expression of MMP9 in the NomoH and NomoL subgroups. C, Survival curve showing the prognostic value of MMP9 expression. D, MMP9 expression was positively associated with macrophage infiltration. E, Immunohistochemistry under different magnifications showing remarkably upregulated MMP9 in the NomoH subgroup.

There is an attractive clinical value of accurately predicting the efficacy of pharmacotherapeutic management since it is an important and costly way to reduce tumour size and maximize OS time, but relatively low response rates are a limitation. After estimating the precision of the IC_{50} for pazapanib, temsirolimus, and rapamycin of each group by our predictive score model, dramatic differences were recognized among groups (Fig. 5D). Patients in the NomoL subgroup seemed to better react to treatment with pazapanib (P = 0.017), temsirolimus (P = 0.008) and rapamycin (P = 0.008).

4. Discussion

Although the current OS rates for WT patients have been greatly improved due to various therapies and systematic treatment strategies, the toxicity and secondary cancerogenic effects originating from nonspecified targets remain issues to be resolved [31]. TIICs admixed with mesenchymal cells and extracellular matrix are critical components relevant in the tumour microenvironment [32,33], and these cells could be promising candidates for the diagnosis, prognosis, and identification of individualized immunotherapy targets by altering tumour dissemination, metastasis, relapse, and therapeutic response [34,35]. Previous research has focused more on the presence and localization of specific TIICs

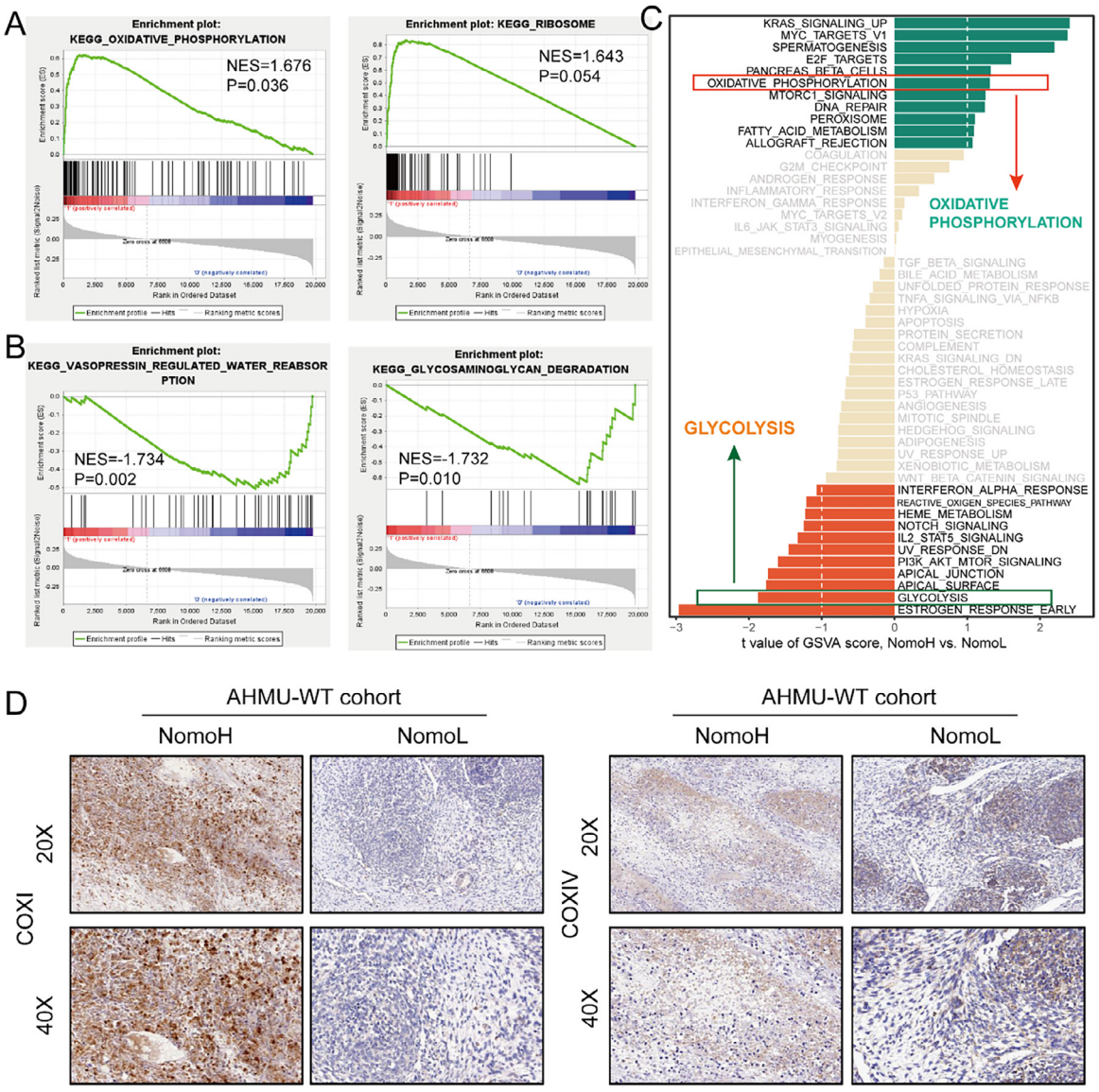

Fig. 4. Identification of functions and pathways related to WT prognosis. A, B, GSEA demonstrating the most highly enriched pathways. C, GSVA showing the activated oxidative phosphorylation and glycolysis pathways. D, Immunohistochemistry staining under different magnifications showing remarkably high expression of COX1 and relatively high expression of COX4 in the NomoH subgroup.

qualitatively by detecting fewer specific targets and limited markers in the same patient samples [10–13], leading to repetitive computation and finally encompassing a vision of the immune cell landscape.

In our study, we analysed the gene expression profile and clinical information from 130 wt patients and 6 healthy controls to establish a methodology and quantified the tumour immune milieu more comprehensively than previous studies. $CD4^+$ T cells, dendritic cells, neutrophils, NK cells, and regulatory T cells were highly present in normal tissues, while infiltrated macrophages were more abundant in WT samples than in normal tissues. Our results indicated that a lower level of infiltrated monocytes and a higher level of macrophages were correlated with the poor prognosis of WT patients. TAMs, differentiated from monocytes, promote malignant cell survival and proliferation while inhibiting cytotoxic T cell activity [36–38]. The relationship between macrophage recruitment and WT progression was first found by Liou et al. [39]. Macrophages were regarded as the most predominant immune-stained macrophages in the WT stroma, with an inflammatory marker called cyclooxygenase-2 (COX-2) robustly expressed. [14] Recently, Tian et al. observed that TAMs were recruited and located to the tumour stroma and polarized towards proinflammatory classical activated macrophages (M1) or suppressive alternatively activated (M2) macrophages. After analysing the density and quantity of various macrophages with tumour stages, patients with more M2 macrophages had an unfavourable prognosis with shorter OS time and higher mortality rates [40]. Fiore et al. followed up this research and showed that the recruited M2 subsets (MR, CD206) could blunt the production of IFN by NK cells in different ways and weaken the function of NK activity by M2-NK contact. In line with Tian et al.'s research, a lack of CD80 and CCR7 polarization could also be found, indicating a decreasing quantity of M1 along with the advanced stage. In this context, they also validated that higher expression of ID4 could be used as an indicator to evaluate clinical outcomes [41]. Our results are consistent with those found in the monocyte-to-macrophage polarization process and WT tumour stages, which is why we included monocytes and macrophages as prognostic prediction factors.

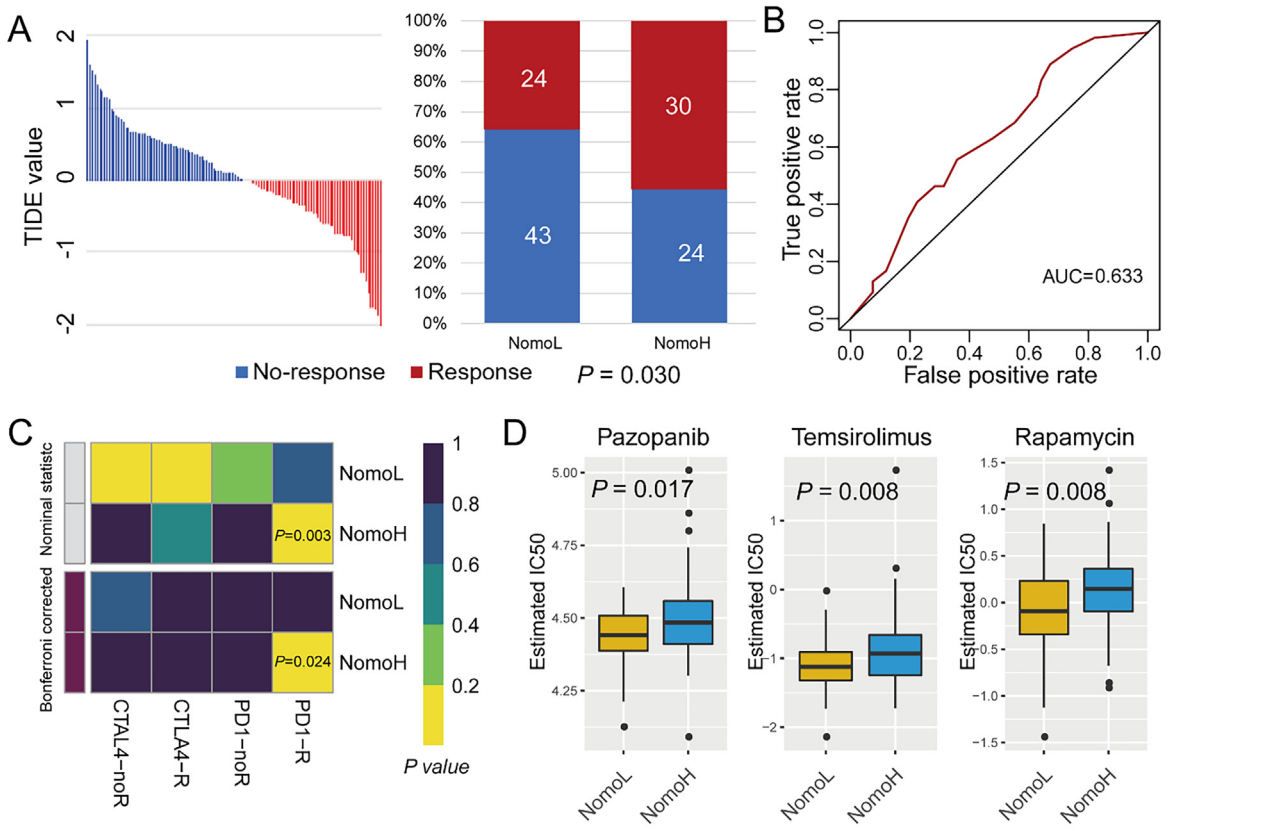

Fig. 5. Immunotherapy and chemotherapy strategy for WT patients. A, TIDE value and response results to immunotherapies of patients in the NomoH and NomoL subgroups. B, ROC curve analysis was performed to assess the predictive performance of the nomogram points for immunotherapy response. C, Subclass analysis to predict the response to anti-CTAL4/PD-1 therapy. D, Estimation of the reaction to pazopanib, temsirolimus and rapamycin.

In the second part of the study, we integrated multiple prognostic factors, including the overall landscape of TIICs, to establish a nomogram model and provide a precise and individualized prediction of the 3- and 5-year OS. Previous research only focused on a few single variables, such as tumour stage or histology, to judge the prognosis and outcome of WT patients, which could inevitably lead to deviation. To eliminate bias, we included sex, stage, monocytes, and macrophages to calculate the final point value. It is worth mentioning that patients' sex was not considered a significant prognostic factor due to the relatively equivalent distribution in males and females in previous studies [1,42]. However, in our research, sex was an independent factor that showed statistical significance in the Cox regression analysis. According to previous studies, different classifications of age led to different outcomes due to the lack of shared criteria [42], whereas patient age was not a statistically significant parameter in our study. Although the H-L test and AUCs demonstrated satisfactory discriminative performance in both the validation database and the patients enrolled by us, the different roles sex and age played might be selective bias based on data shapes provided by the TARGET-WT project.

A higher point value calculated by the nomogram model we developed was positively associated with a poor prognosis; however, the detailed mechanism between monocyte-to-macrophage polarization, macrophage infiltration, and poor prognosis remained unclear. Therefore, we evaluated the DEGs and potential pathways, and then we investigated the results experimentally. The findings suggested that a higher level of MMP9 expression was relevant to a worse survival probability. It has been widely confirmed that MMP9, mainly secreted by TAMs [43], has a direct or indirect association with several tumour types, including WT [43–46]. Wang et al. showed that mono-2-ethyhexyl phthalate could result in the migration and invasion of WT cells in vitro through MMP2/9 and finally activate carcinoma progression via the NF-kB pathway [45]. Jia et al. reported that curcumin could downregulate MMP2/9 expression by inhibiting RECK methylation, which blunted the tumorigenicity, invasion, and metastasis ability of WT in vitro and in vivo [46]. Meanwhile, NLR, PLR and SII have been extensively proven to have high value in the assessment as prognostic biomarkers among different diseases [47–49], and our study is the first to reveal that increased inflammatory factors have predictive value among patients with severe WT. GSEA/GSVA demonstrated that the most highly enriched hub genes were closely related to activated oxidative phosphorylation. As a vital part of metabolism supporting high proliferation, the Warburg effect serves as a fundamental metabolic approach to generate ATP in tumour cells. The high activity of cytochrome *C* oxidase (COX), which plays a central role in the regulation of the cellular metabolism process, is now well established as a biomarker to detect oxidative phosphorylation [50,51]. This is also the first study to investigate the association between COX1/4 and WT, and our results demonstrated a high level of metabolism due to a high expression of COX1/4.

Our ultimate goal is to offer advantages to patients with existing therapies. Therefore, in the last part of our study, the ability of our nomogram to evaluate the reaction to traditional chemotherapeutics and immune therapies was estimated. Apart from traditional chemotherapeutics, PD1/PDL1 and CTLA-4 therapy are innovative applications for immunotherapy. Based on the successes of antibodies targeting PD1/PDL1 and CTLA-4, immunotherapies are now available in clinical application for the treatment of patients with various tumours [52,53], despite resistance to novel

blockers in some solid tumours. [54] Until now, the application of those blockers in WT patients has not been reported. Since the best potential therapy should be available for WT patients, considering the lower-than-expected efficacy and safety, it is necessary to develop biomarkers for predicting patients' responses to these therapies. Our analysis indicated the similarity of the expression profile between WT in the NomoH subgroup and melanoma patients responding to anti-PD1 therapy, indicating the potential value of anti-PD1 therapy in WT. Additionally, patients in the NomoL subgroup obtained lower predicted IC_{50} scores, reflecting their response to chemotherapy and demonstrating the advantage of our model in guiding clinical therapy strategies for different WT patients.

At the same time, some limitations should also be addressed and modified in future studies. First, the TARGET-WT cohort only enrolled the relapsed FHWT cases, along with the DAWT cases, therefore, that's why we did not observed the device OS in these two histology subtypes, further study with no-relapsed FHWT cases is needed to validation the predict value of immunocytes in WT. Second, the nomogram model was built upon the gene expression profile and clinical information from the TARGET-WT project and validated by the 7 patients from AHMU-WT cohort. The selective bias based on data shapes might be caused by a limited number of samples, which suggests that more WT patients and databases should be used to validate the effectiveness of our model. Thrid, the comprehensive landscape of TIICs was constructed based on computational calculations, so more studies should be carried out elucidating the potential mechanism by which a lower level of infiltrated monocytes and a higher level of macrophages are associated with the prognosis of WT. Forth, if the nomogram model applied in the clinical, each institute need to construct a baseline cohort to confirm the median cut-off value, no matter used the IHC staining H-score, or the CIBERSORT results from RNA-sequence, due to the impact of different methods, equipment and population.

5. Conclusion

In summary, we first described a comprehensive TIIC landscape in WT by applying the deconvolution algorithm of CIBERSORT and demonstrated that a higher proportion of macrophages and lower levels of monocytes were related to an unfavourable prognosis. Based on what we have learned about the immune landscape, we first established and validated a nomogram model to predict the prognosis of WT cases containing both TIICs and some significant clinical factors, and we also linked the activated oxidative phosphorylation pathway with a poor prognosis of WT patients.

6. Ethics approval

For the AHMU-WT cohort, the research contents and programs were reviewed and approved by the Ethics Committee of the First Affiliated Hospital of Anhui Medical University (PJ2021-01-25), and patient consent for the retrospective cohorts was waived. The study methodologies conformed to the standards set by the Declaration of Helsinki.

Declaration of Competing Interest

The authors declare that they have no known competing financial interests or personal relationships that could have appeared to influence the work reported in this paper.

Acknowledgements

This work was supported by the National Natural Science Foundation of China [grant number: 81972539, U1732157, 82170787, 81870519, 81630019]; Scientific Research Foundation of the Institute for Translational Medicine of Anhui Province [grant number: 2017ZHYX02]; The Key Project of Provincial Natural Science Research Project of Anhui Colleges [grant number: KJ2019A0278].

Author contributions

JLM, JD conceived and designed the research; YHC, XFL, QTG and CZL performed the date record and collection; JLM, YHC and XFL conducted the data analysis and visualization; JLM, YHC, JD and CZL wrote and review the manuscript. All authors read and approved the final manuscript.

Data availability

All the data used in this study are publicly available as described in the Methods section. The data behind the figures are available in the supplementary data. The other data will be available from the corresponding author upon request.

Appendix A. Supplementary data

Supplementary data to this article can be found online at https://doi.org/10.1016/j.csbj.2022.06.052.

References

[1] Cunningham ME, Klug TD, Nuchtern JG, Chintagumpala MM, Venkatramani R, Lubega J, et al. Global disparities in wilms tumor. J Surg Res 2020;247:34–51.
[2] Chu A, Heck JE, Ribeiro KB, Brennan P, Boffetta P, Buffler P, et al. Wilms' tumour: a systematic review of risk factors and meta-analysis. Paediatr Perinat Epidemiol 2010;24(5):449–69.
[3] Stiller CA, Parkin DM. International variations in the incidence of childhood renal tumours. Br J Cancer 1990;62(6):1026–30.
[4] Leslie SW, Sajjad H, Murphy PB. Wilms Tumor. StatPearls Treasure Island (FL) 2020.
[5] Liu EK, Suson KD. Syndromic Wilms tumor: a review of predisposing conditions, surveillance and treatment. Transl Androl Urol 2020;9(5):2370–81.
[6] Scott RH, Stiller CA, Walker L, Rahman N. Syndromes and constitutional chromosomal abnormalities associated with Wilms tumour. J Med Genet 2006;43(9):705–15.
[7] Malogolowkin M, Cotton CA, Green DM, Breslow NE, Perlman E, Miser J, et al. Treatment of Wilms tumor relapsing after initial treatment with vincristine, actinomycin D, and doxorubicin. A report from the National Wilms Tumor Study Group. Pediatr Blood Cancer 2008;50(2):236–41.
[8] Aldrink JH, Heaton TE, Dasgupta R, Lautz TB, Malek MM, Abdessalam SF, et al. Update on Wilms tumor. J Pediatr Surg 2019;54(3):390–7.
[9] Jereb B, Diehl V, Ahstrom L, Juhlin I. Relation between cellular immunity to nephroblastoma and the phase of the disease. Acta Paediatr Scand 1972;61(6):709–14.
[10] Nagai K, Yamada A, Eguchi H, Kato H, Itoh K. HLA-A2402-restricted and tumor-specific cytotoxic T lymphocytes from tumor-infiltrating lymphocytes of a child with Wilms' tumor. Pediatr Res 1997;42(1):122–7.
[11] Vakkila J, Jaffe R, Michelow M, Lotze MT. Pediatric cancers are infiltrated predominantly by macrophages and contain a paucity of dendritic cells: a major nosologic difference with adult tumors. Clin Cancer Res 2006;12(7 Pt 1):2049–54.
[12] Holl EK, Routh JC, Johnston AW, Frazier V, Rice HE, Tracy ET, et al. Immune expression in children with Wilms tumor: a pilot study. J Pediatr Urol 2019;15(5):441 e1–e8.
[13] Mardanpour K, Rahbar M, Mardanpour S, Mardanpour N, Rezaei M. CD8+ T-cell lymphocytes infiltration predict clinical outcomes in Wilms' tumor. Tumour Biol 2020;42(12):1010428320975976.
[14] Maturu P, Overwijk WW, Hicks J, Ekmekcioglu S, Grimm EA, Huff V. Characterization of the inflammatory microenvironment and identification of potential therapeutic targets in wilms tumors. Transl Oncol 2014;7(4):484–92.
[15] Maturu P. The Inflammatory Microenvironment in Wilms Tumors. In: van den Heuvel-Eibrink MM, editor. Wilms Tumor. Brisbane (AU)2016.
[16] Newman AM, Liu CL, Green MR, Gentles AJ, Feng W, Xu Y, et al. Robust enumeration of cell subsets from tissue expression profiles. Nat Methods 2015;12(5):453–7.

[17] Gadd S, Huff V, Walz AL, Ooms A, Armstrong AE, Gerhard DS, et al. A Children's Oncology Group and TARGET initiative exploring the genetic landscape of Wilms tumor. Nat Genet 2017;49(10):1487–94.
[18] Subramanian A, Tamayo P, Mootha VK, Mukherjee S, Ebert BL, Gillette MA, et al. Gene set enrichment analysis: a knowledge-based approach for interpreting genome-wide expression profiles. Proc Natl Acad Sci U S A 2005;102(43):15545–50.
[19] Hoshida Y, Brunet JP, Tamayo P, Golub TR, Mesirov JP. Subclass mapping: identifying common subtypes in independent disease data sets. PLoS ONE 2007;2(11):e1195.
[20] Lu X, Jiang L, Zhang L, Zhu Y, Hu W, Wang J, et al. Immune signature-based subtypes of cervical squamous cell carcinoma tightly associated with human papillomavirus type 16 expression, molecular features, and clinical outcome. Neoplasia 2019;21(6):591–601.
[21] Roh W, Chen PL, Reuben A, Spencer CN, Prieto PA, Miller JP, et al. Integrated molecular analysis of tumor biopsies on sequential CTLA-4 and PD-1 blockade reveals markers of response and resistance. Sci Transl Med 2017;9(379).
[22] Geeleher P, Cox NJ, Huang RS. Clinical drug response can be predicted using baseline gene expression levels and in vitro drug sensitivity in cell lines. Genome Biol 2014;15(3):R47.
[23] Gantzel RH, Kjaer MB, Laursen TL, Kazankov K, George J, Moller HJ, et al. Macrophage activation markers, soluble CD163 and Mannose receptor, in liver fibrosis. Front Med (Lausanne) 2020;7:615599.
[24] Zhao SX, Li WC, Fu N, Kong LB, Zhang QS, Han F, et al. CD14(+) monocytes and CD163(+) macrophages correlate with the severity of liver fibrosis in patients with chronic hepatitis C. Exp Ther Med 2020;20(6):228.
[25] Hiatt J, Cavero DA, McGregor MJ, Zheng W, Budzik JM, Roth TL, et al. Efficient generation of isogenic primary human myeloid cells using CRISPR-Cas9 ribonucleoproteins. Cell Rep 2021;35(6):109105.
[26] Fageeh HI, Fageeh HN, Patil S. Monocyte differentiation into destructive macrophages on in vitro administration of gingival crevicular fluid from periodontitis patients. J Pers Med 2021;11(6).
[27] Cybularz M, Wydra S, Berndt K, Poitz DM, Barthel P, Alkouri A, et al. Frailty is associated with chronic inflammation and pro-inflammatory monocyte subpopulations. Exp Gerontol 2021;149:111317.
[28] Yin Y, Xu L, Chang Y, Zeng T, Chen X, Wang A, et al. N-Myc promotes therapeutic resistance development of neuroendocrine prostate cancer by differentially regulating miR-421/ATM pathway. Mol Cancer 2019;18(1):11.
[29] Chen J, Zhan C, Zhang L, Zhang L, Liu Y, Zhang Y, et al. The hypermethylation of Foxp3 promoter impairs the function of Treg cells in EAP. Inflammation 2019;42(5):1705–18.
[30] Schneider CA, Rasband WS, Eliceiri KW. NIH Image to ImageJ: 25 years of image analysis. Nat Methods 2012;9(7):671–5.
[31] Lopes RI, Lorenzo A. Recent advances in the management of Wilms' tumor. F1000Res 2017;6:670.
[32] Puram SV, Tirosh I, Parikh AS, Patel AP, Yizhak K, Gillespie S, et al. Single-cell transcriptomic analysis of primary and metastatic tumor ecosystems in head and neck cancer. Cell 2017;171(7):1611–24 e24.
[33] Jung HY, Fattet L, Yang J. Molecular pathways: linking tumor microenvironment to epithelial-mesenchymal transition in metastasis. Clin Cancer Res 2015;21(5):962–8.
[34] Zeng D, Zhou R, Yu Y, Luo Y, Zhang J, Sun H, et al. Gene expression profiles for a prognostic immunoscore in gastric cancer. Br J Surg 2018;105(10):1338–48.
[35] Gentles AJ, Newman AM, Liu CL, Bratman SV, Feng W, Kim D, et al. The prognostic landscape of genes and infiltrating immune cells across human cancers. Nat Med 2015;21(8):938–45.
[36] Qian BZ, Pollard JW. Macrophage diversity enhances tumor progression and metastasis. Cell 2010;141(1):39–51.
[37] Ruffell B, Affara NI, Coussens LM. Differential macrophage programming in the tumor microenvironment. Trends Immunol 2012;33(3):119–26.
[38] Meng J, Liu Y, Guan S, Fan S, Zhou J, Zhang M, et al. The establishment of immune infiltration based novel recurrence predicting nomogram in prostate cancer. Cancer Med 2019;8(11):5202–13.
[39] Liou P, Bader L, Wang A, Yamashiro D, Kandel JJ. Correlation of tumor-associated macrophages and clinicopathological factors in Wilms tumor. Vasc Cell 2013;5(1):5.
[40] Tian K, Wang X, Wu Y, Wu X, Du G, Liu W, et al. Relationship of tumour-associated macrophages with poor prognosis in Wilms' tumour. J Pediatr Urol 2020;16(3). 376 e1–e8.
[41] Fiore PF, Vacca P, Tumino N, Besi F, Pelosi A, Munari E, et al. Wilms' tumor primary cells display potent immunoregulatory properties on NK cells and macrophages. Cancers (Basel) 2021;13(2).
[42] Tang F, Zhang H, Lu Z, Wang J, He C, He Z. Prognostic factors and nomograms to predict overall and cancer-specific survival for children with wilms' tumor. Dis Markers 2019;2019:1092769.
[43] Riabov V, Gudima A, Wang N, Mickley A, Orekhov A, Kzhyshkowska J. Role of tumor associated macrophages in tumor angiogenesis and lymphangiogenesis. Front Physiol 2014;5:75.
[44] Huang H. Matrix metalloproteinase-9 (MMP-9) as a cancer biomarker and MMP-9 biosensors: recent advances. Sensors (Basel) 2018;18(10).
[45] Wang Z, Shao M, Liu Y. Promotion of Wilms' tumor cells migration and invasion by mono-2-ethyhexyl phthalate (MEHP) via activation of NF-kappaB signals. Chem Biol Interact 2017;270:1–8.
[46] Jia W, Deng F, Fu W, Hu J, Chen G, Gao X, et al. Curcumin suppresses wilms' tumor metastasis by inhibiting RECK methylation. Biomed Pharmacother 2019;111:1204–12.
[47] Ponti G, Maccaferri M, Ruini C, Tomasi A, Ozben T. Biomarkers associated with COVID-19 disease progression. Crit Rev Clin Lab Sci 2020;57(6):389–99.
[48] Wang Q, Ma J, Jiang Z, Ming L. Prognostic value of neutrophil-to-lymphocyte ratio and platelet-to-lymphocyte ratio in acute pulmonary embolism: a systematic review and meta-analysis. Int Angiol 2018;37(1):4–11.
[49] Wang B, Huang Y, Lin T. Prognostic impact of elevated pre-treatment systemic immune-inflammation index (SII) in hepatocellular carcinoma: A meta-analysis. Medicine (Baltimore) 2020;99(1):e18571.
[50] Aminzadeh S, Vidali S, Sperl W, Kofler B, Feichtinger RG. Energy metabolism in neuroblastoma and Wilms tumor. Transl Pediatr 2015;4(1):20–32.
[51] Lee SY, Jeon HM, Ju MK, Kim CH, Yoon G, Han SI, et al. Wnt/Snail signaling regulates cytochrome C oxidase and glucose metabolism. Cancer Res 2012;72(14):3607–17.
[52] Seliger B. Basis of PD1/PD-L1 therapies. J Clin Med 2019;8(12).
[53] Kambayashi Y, Fujimura T, Hidaka T, Aiba S. Biomarkers for predicting efficacies of anti-PD1 antibodies. Front Med (Lausanne) 2019;6:174.
[54] Lei Q, Wang D, Sun K, Wang L, Zhang Y. Resistance mechanisms of anti-PD1/PDL1 therapy in solid tumors. Front Cell Dev Biol 2020;8:672.